Chapter 4

FLUX CALCULATIONS

4.1. Introduction

The sediments are one of the sources of alkalinity to the overlying lakewater. The rate at which sediments are contributing alkalinity must be known, along with the rate at which other watershed sources are contributing alkalinity to the lakewater, in order for the Air Resources Board to set a deposition standard which will protect sensitive Sierran Lakes. The solid phase data presented in Chapter 2 and the porewater profiles presented in the last chapter provide a means of calculating the fluxes between the sediments and the overlying water. This chapter is concerned with making these calculations and comparing the results with other methods of flux determination.

The rest of this introductory section presents a discussion of the theory of flux calculations and the methods we used to do these calculations. Considerable space is devoted to two phenomena that affect calculations of molecular diffusion: activity coefficient gradients and electrical forces. Some circumstances allow one to ignore these effects, and many workers have ignored one or both. We do the calculations with and without these refinements, so one of the results of this chapter is a determination of whether and when these effects are important.

Flux is the rate of transfer of material between two regions, in this study, the sediments and the overlying water, or,

identically, across some boundary, usually the sediment-water interface. Fluxes occur by one or a combination of three mechanisms: advection, turbulent diffusion, and molecular diffusion (Lerman 1979 p. 42). The total flux, J, is the sum of these three fluxes:

$$J = J_a + J_{td} + J_{md}$$

We assume, as is common for sediment systems, that vertical fluxes dominate and horizontal fluxes can be ignored.

4.1.1. Advective flux

A flux of either solutes or water resulting from the mass flow of water is termed an advective flux. It is the product of a density or concentration and the velocity of the mass flow:

$$J_{a,i} = \phi C_i v$$

where $J_{a,i}$ is the advective flux of the ith species per unit area of total sediment, C_i is the concentration of the ith species in the liquid phase, v is the velocity of mass flow, and $0 \leq \phi \leq 1$ is the effective porosity, the ratio of the volume of the interconnected pore space to the volume of the total sediment.[1] The flux

[1] Only interconnected pores are included, because isolated pores are not available channels for transport. Isolated pores are assumed to be rare in shallow sediments (Berner 1980, p. 16). However, problems may arise if they are not rare, because porosity is measured by comparing wet and dry weights of sediment. In highly organic sediments, water trapped in isolated pore spaces may evaporate, yielding a total porosity which is considerably greater than effective porosity. A reported example that may be explained by this hypothesis are some highly organic (20%-30% organic carbon) and highly porous (96%) cores that nontheless had measured tortuosities (see below) of about 0.6 (Rudd et al. 1986).

is less in a porous medium because the velocity moves the dissolved substance only through pore spaces, while the units of flux are mass per unit area of total sediment per unit time.[2]

4.1.2. Turbulent diffusive flux: eddy diffusion and dispersion

Diffusion is transport down a concentration gradient due to random motion. Turbulent diffusion results from the "random" movement of parcels of water of larger than molecular scale. On a very small scale, turbulent diffusion appears advective, but viewed from a large enough scale, it can be modeled as a random process, and it results in a net flux only if there is a concentration gradient.

$$J_{td,i} = -\phi D_{td} \frac{\partial C_i}{\partial x}$$

where $J_{td,i}$ is the turbulent diffusive flux of the ith species, D_{td} is the turbulent diffusion coefficient, and x is vertical distance increasing downwards. The negative sign indicates that the flux occurs in the in the direction of decreasing concentration. Turbulent diffusion in open water is usually caused by currents and is termed eddy diffusion.

Another process usually modeled with an equation of this form is porewater dispersion and results from the advective flux of water and solutes through porous media. This kind of mixing is

[2] Bear (1972, p. 22) has shown that areal porosity and volume porosity are identical, regardless of pore geometry and even for anisotropic porosity distributions. This fact is important because porosities are measured as volume porosities, while the porosity in the flux equation is an areal porosity.

caused by velocity gradients resulting from friction with the pore walls. Like eddy diffusion, dispersion does not look random on a microscopic scale, but on a larger scale it is well approximated as a diffusive process.

4.1.3. Molecular diffusive fluxes

Molecular diffusion is caused by the random motion of molecules. Strictly speaking, molecular diffusion occurs down the chemical potential gradient, rather than the concentration gradient (Denbigh 1981, p. 86). The following one-dimensional development follows Lasaga (1979) and assumes that the diffusing species are ions. It applies equally well to neutral molecules, however, since the effect of the diffusion potential disappears when multiplied by the charge (zero) of a neutral molecule. This development is included to assist the interested reader in understanding where equation (16) comes from, but may also be skipped, except to pick up the definitions of some terms.

The force on the ith ion, F_i, can be thought of as having a thermodynamic component, the gradient in chemical potential ($\nabla\mu_i$), and an electrical component, the charge on the ion (z_i) times the gradient in electrical potential (∇E).[3] The electrical potential, called the diffusion potential, results from the diffusion of ions with different diffusion coefficients. The effect of the electrical potential, indeed its essential mathematical

[3] ∇ is shorthand for gradient. Since we are considering gradients in the vertical (x) direction only, $\nabla C = \partial C/\partial x$, $\nabla E = \partial E/\partial x$, etc.

property, is the preservation of macroscopic electroneutrality. The force on ion i is then

$$F_i = -\nabla\mu_i + z_i \nabla E$$

The molecular diffusive flux of ion i results from this force:

$$J_{md,i} = \phi C_i u_i F_i$$

where u_i is the limiting velocity due to a unit force on the ith species in the solvent environment. Substituting for F_i,

$$J_{md,i} = -\phi u_i C_i \nabla\mu_i + \phi u_i z_i C_i \nabla E \tag{1}$$

For this equation to be useful, u_i, $\nabla\mu_i$, and ∇E must be converted into expressions involving terms available from my measurements or the literature: concentration gradients, activity coefficient gradients, and diffusion coefficients. To facilitate this conversion, we define two new variables:

$$A_i = -\phi u_i C_i \nabla\mu_i \tag{2}$$

and

$$B_i = \phi u_i z_i C_i \nabla E \tag{3}$$

so that

$$J_{md,i} = A_i + B_i \tag{4}$$

A_i is the flux due to the chemical potential and B_i is the flux due to the diffusion potential. The chemical potential is expressed is as follows (Stumm and Morgan 1981, p.42):

$$\mu_i = \mu_i^\circ + RT\ln(a_i) \tag{5}$$

where where μ_i° is the chemical potential at some standard state,

R is the gas constant, T is the absolute temperature, and a_i is the activity, which is defined to be equal to concentration at infinite dilution. In a real solution, it is related to concentration by the activity coeffcient, γ_i:[4]

$$a_i = \gamma_i C_i \tag{6}$$

Substituting for a_i and differentiating equation (5) with respect to depth (x) gives the following expression for the gradient of the chemical potential:

$$\frac{\partial \mu_i}{\partial x} = \frac{RT}{\gamma_i}\frac{\partial \gamma_i}{\partial x} + \frac{RT}{C_i}\frac{\partial C_i}{\partial x} \tag{7}$$

Substituting equation (7) into equation (2) gives

$$A_i = -\phi u_i C_i \frac{RT}{\gamma_i}\frac{\partial \gamma_i}{\partial x} - \phi u_i RT \frac{\partial C_i}{\partial x} \tag{8}$$

The Nearnst-Einstein equation, which relates diffusion coefficients, D_i, to ionic mobilities,

$$D_i = RTu_i \tag{9}$$

allows the substitution in equation (8) of the diffusion coefficient, D_i, for RTu_i, giving

---

[4] Activity coefficients are approximated as a function of ionic strength, I, which is defined as $I=0.5\sum_{i=1}^{n} z_i^2 C_i$ for a solution containing n species.
We are using the Guntelberg approximation for activity coefficients (Stumm and Morgan 1981, p. 135): $\log \gamma_i = -0.5 z_i^2 \frac{\sqrt{I}}{1+\sqrt{I}}$

$$A_i = -\phi D_i \left(\frac{C_i}{\gamma_i} \frac{\partial \gamma_i}{\partial x} + \frac{\partial C_i}{\partial x} \right) \tag{10}$$

This expression for the portion of the molecular diffusive flux due to the chemical potential includes both concentration and activity-coefficient gradients. If the activity-coefficient gradient is zero, this expression reduces to the familiar form of Fick's first law in which the flux is equal to a constant times the concentration gradient.

The next step is to obtain an expression for B_i, the molecular diffusive flux of ion i due to the diffusion potential. For a system containing n species, electrical neutrality requires that

$$\sum_{j=1}^{n} z_j J_{md,j} = 0 \tag{11}$$

Substituting for $J_{md,j}$ from equation (4) gives

$$\sum_{j=1}^{n} z_j A_j + \sum_{j=1}^{n} z_j B_j = 0$$

Substituting for B_i from equation (3) gives

$$\sum_{j=1}^{n} z_j A_j + \sum_{j=1}^{n} \phi u_j z_j^2 C_j \nabla E = 0 \tag{12}$$

Solving for ∇E gives

$$\nabla E = \frac{-\sum_{j=1}^{n} z_j A_j}{\phi \sum_{j=1}^{n} z_j^2 u_j C_j} \tag{13}$$

Substituting this expression for ∇E into equation (3) gives

$$B_i = -\phi u_i z_i C_i \frac{\sum_{j=1}^{n} z_j A_j}{\phi \sum_{j=1}^{n} z_j^2 u_j C_j} \tag{14}$$

If the right side of this equation is multiplied by RT/RT and the Nernst-Einstein equation, (9), is used to substitute D_i's for RTu_i's, then

$$B_i = -\phi D_i z_i C_i \frac{\sum_{j=1}^{n} z_j A_j}{\phi \sum_{j=1}^{n} z_j^2 D_j C_j} \tag{15}$$

This expression for the molecular diffusive flux of ion i due to the diffusion potential can be understood as follows: The summation in the numerator is the charge imbalance that would result from diffusion of all species with no correction for the diffusion potential. The remainder of the expression apportions to the ith species a fraction of this total charge imbalance according to the charge, concentration, and diffusion coefficient of the ith species.

There is one remaining correction to be applied to the diffusive flux equation for an ion in a porous medium: the tortuosity factor, T. This is a factor between zero and one that reduces the diffusion coefficient for an ion or molecule in a non-porous medium, D_i, to account for the tortuous path it must take in a porous medium.[5]

[5] Tortuosity is discussed more fully below.

$$D_{i,s} = TD_i$$

where $D_{i,s}$ is referred to as the whole-sediment diffusion coeff-cient for ion i.

After substituting equations (10) for A_i and (15) for B_i into equation (4) and including the tortuosity correction, the final expression for the flux due to molecular diffusion in a porous medium is

$$J_{md,i} = -\phi TD_i \left(\frac{C_i}{\gamma_i} \frac{\partial \gamma_i}{\partial x} + \frac{\partial C_i}{\partial x} \right) + \frac{\phi TD_i z_i C_i}{\sum_{j=1}^{n} z_j^2 C_j D_j} \sum_{j=1}^{n} z_j D_j \left(\frac{C_j}{\gamma_j} \frac{\partial \gamma_j}{\partial x} + \frac{\partial C_j}{\partial x} \right) \quad (16)$$

Note that the tortuosities and porosities associated with the summation terms cancelled each other out.

If there is a negligible gradient in ionic strength, then $\nabla \gamma_i = 0$, and equation (16) reduces to the following simpler form:

$$J_{md,i} = -\phi TD_i \frac{\partial C_i}{\partial x} + \frac{\phi TD_i z_i C_i}{\sum_{j=1}^{n} z_j^2 C_j D_j} \sum_{j=1}^{n} z_j D_j \frac{\partial C_j}{\partial x} \quad (17)$$

While Lasaga acknowledges that his method of handling the diffusion potential is an approximation, it can be shown by substituting either equation (16) or (17) into equation (11) that this method does result in macroscopic charge balance, as must be the case physically.

Tortuosity

The tortuosity factor, T, decreases the diffusion coefficient because of the tortuous path a diffusing molecule must take in a porous medium as a result of its geometry. Different authors treat this factor differently, depending on their interpretation of its physical meaning. We follow Bear's (1972) usage in considering it a multiplicative coefficient:

$$D_{i,s} = TD_i$$

where $D_{i,s}$ is the diffusion coefficient of ion i in the sediment, $0 \leq T \leq 1$ is the tortuosity factor, and D_i is the diffusion coefficient in homogeneous aqueous solution. This equation can be converted into an operational definition of the tortuosity factor:

$$T = \frac{D_{i,s}}{D_i}$$

Unfortunately, to use this equation one must measure $D_{i,s}$. If $D_{i,s}$ were measured, there would be no need to know T. Since $D_{i,s}$ was not measured, some estimate of T is necessary.

Most authors have attempted to express the tortuosity factor as a function of porosity. This approach is intuitively appealing: In a nonporous solution, both the porosity and the tortuosity factor are equal to one. As the porosity decreases, more of the medium is taken up by solid particles, and the tortuosity factor should also decrease. Such a functional relationship is also useful, because porosity is a common and easy-to-make measurement. Most authors have chosen to use the relationship

$$T = \phi^n$$

Various authors have found such an empirical function for a given sediment, but, unfortunately, the function varies widely between sediments for reasons that are not clear.[6] There may be a large difference between the particle geometries of different sediments; there may also be a large component of measurement error. We use Lerman's (1979, p. 92) suggestion, that, in the absence of a better model, $T=\phi^2$. This function is close to what a number of authors have found for fine-grained sediments, but it remains a source of considerable uncertainty in flux calculations.

Temperature corrections for molecular diffusion coefficients

The diffusion coefficients used in equations (16) and (17) are infinite-dilution tracer or self-diffusion coefficients, which are measured by experimental setups that allow the measurement of ionic mobility in a way that decouples or subtracts the influence of other ions. The influence of ionic strength on D is relatively small (Lasaga 1979, Li and Gregory 1974, Krom and Berner 1980). The greatest influence on D is the viscosity of the solution, which results to a small degree from dissolved substances (the viscosity of seawater is about 8% greater than that of freshwater), but primarily from temperature: the viscosity of

[6] For examples, see Andrews and Bennett (1981), McDuff and Gieskes (1976), Kepkay et al. (1981), Hesslein (1980), Krom and Berner (1980), Li and Gregory (1974), Rudd et al. (1986), Berner (1980, p.37), Bear (1972, p. 112), Freeze and Cheery (1979, p.104), Thibodeaux (1979, p. 247).

Table 1. Molecular diffusion coefficients at 0°C and 25°C

Species	Diffusion coefficient ($10^{-6}cm^2sec^{-1}$)		References and notes
	0°C	25°C	
Cl^-	10.1	20.3	a
NO_2^-	9.83	19.1	a
Br^-	10.5	20.1	a
NO_3^-	9.78	19.0	a
SO_4^{2-}	5.00	10.7	a
Ca^{2+}	3.73	7.93	a
Mg^{2+}	3.56	7.05	a
Fe^{2+}	3.41	7.19	a
Mn^{2+}	3.05	6.88	a
Na^+	6.27	13.3	a
NH_4^+	9.80	19.8	a
K^+	9.86	19.6	a
CO_2	8.42	19.2	b
CH_4	7.55	17.3	b
H_4SiO_4	10.7	21.5	c
H^+	56.1	93.1	a
OH^-	25.6	52.7	a
HCO_3^-	5.62	11.8	d
$FeHCO_3^+$	4.23	8.50	e
$FeCO_3^0$	2.99	6.00	e
$MnHCO_3^+$	4.23	8.50	e

References and notes:

a. Li and Gregory 1974

b. Lerman 1979, p. 96. Reference supplied values at 5°C and 25°C.

c. Applin 1987. Reference supplied value at 25.5°C.

d. Li and Gregory 1974. Reference supplied value at 25°C.

e. Values taken from similar ions in Applin and Lasaga 1984.

water doubles as the temperature falls from 25°C to 0°C. Between these two temperatures, diffusion coefficients are roughly linear. Therefore, my approach to adjusting diffusion coefficients for temperature has been to compile a table of values at 25°C and 0°C and to linearly interpolate between them. Where measured values were available at the two temperatures, we used those. If values were available at, say, 5°C and 25°C, we linearly extrapolated to 0°C to set up the table. Where values were only available for 25°C, we used the 25°C:0°C ratio of a similar ion to estimate a value for 0°C. Where the ratio for a similar species was not available, we used the ratio of the viscosity of water at the two temperatures, 2.01. The 0°C and 25°C values used to interpolate to the diffusion coefficients used in the flux calculations are presented in Table 1.

4.1.4. The importance of dispersion and advection relative to molecular diffusion

The importance of dispersion relative to molecular diffusion is estimated with the Peclet number, $Pe=dv/TD$, a dimensionless number, where d is particle diameter, v is water velocity, D is the molecular diffusion coefficient, and T is tortuosity. For Peclet numbers less than one, dispersion is considered negligible compared to molecular diffusion (Lerman 1979, p. 65). Using conservative estimates for the sediments of this study ($d=2\mu m$, $TD=3\times10^{-6}cm^2sec^{-1}$), $Pe<1$ implies that $v<13m/day$. Measurements in Emerald Lake (Steve Hamilton, personal communication) and porewater profiles in Eastern Brook and Mosquito Lake indicate that, in

these sediments, v<1mm/day. Since velocities appear to be about four orders of magnitude less than the critical value of 10m/day, dispersion coefficients are assumed to be zero.

The importance of advection relative to molecular diffusion has been examined in the sediment system by looking at porewater profiles for some steady-state solutions generated by a numerical model of advection, diffusion and reaction. Porewater profiles are unaffected by an advective velocity of 0.01mm/day, but are noticeably affected by a velocity of 0.1mm/day. This result is shown in Figure 1 for both positive (downward) and negative (upward) velocity cases.[7] Water velocities resulting from sedimentation in the sediments are less than 1mm/year=0.003mm/day, which are small enough to ignore. It is apparent, however, that what are usually considered very low velocities from a hydrologic-balance point of view could be important velocities in diagenetic modeling.

The effect of these low velocities on fluxes can be examined with some simple calculations. The total flux is the sum of the diffusive and advective fluxes, which, ignoring electrical effects and activity coefficient gradients, is

$$J = -\phi T D \nabla C + \phi C v$$

The relative importance of the diffusive and advective terms may

[7] These model runs used D=1.23cm^{2}day^{-1} and a simple mineral-dissolution expression: dC/dt= 0.0024(417-C) μM day^{-1}. The upper boundary condition was 20μM. Lower boundary condition for the positive velocity case was a rock seal. Lower boundary condition for the negative velocity case was 417μM.

FIG. 1. EFFECT OF ADVECTION ON STEADY STATE SILICA PROFILES

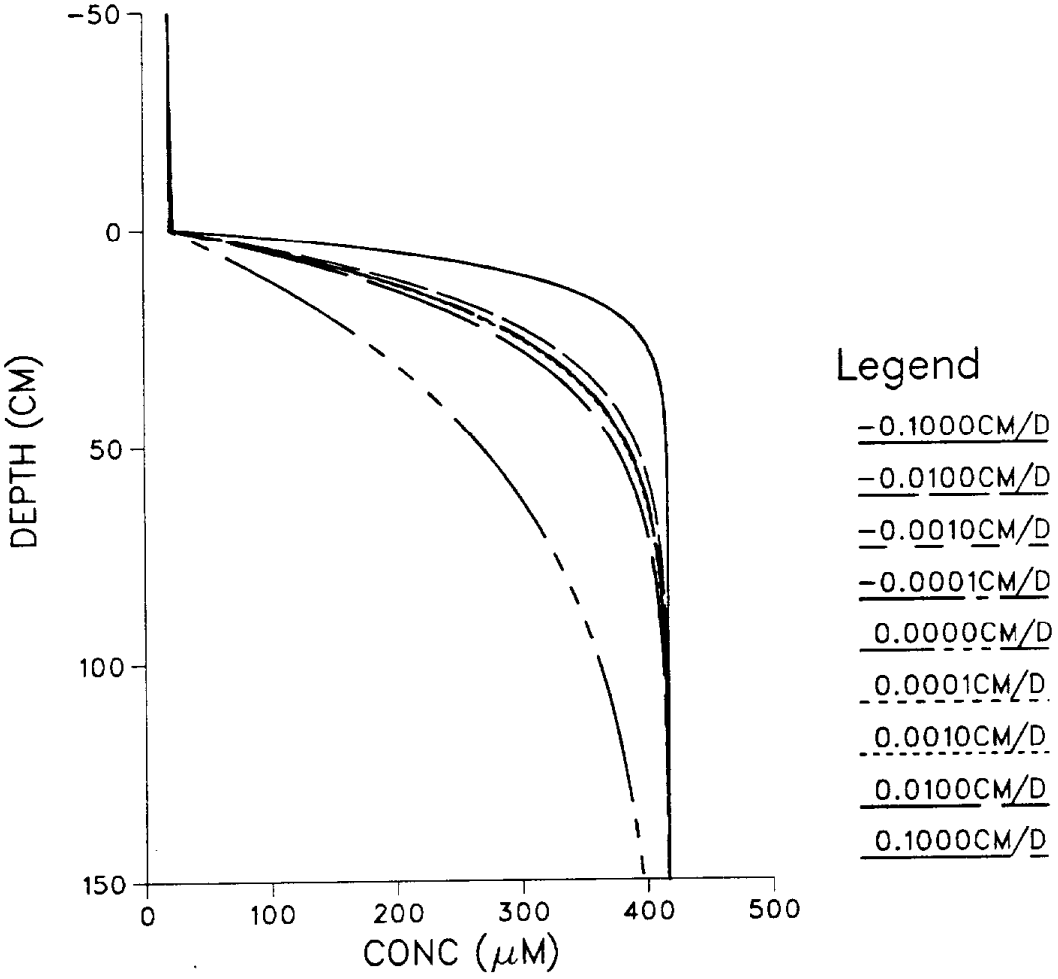

be expressed as a ratio:

$$\frac{Cv}{TD\nabla C}$$

Near the sediment-water interface, gradients and *TD*'s tend to be high and concentration low, while at greater depths in the sediments the reverse is true. Therefore, diffusive flux will tend to be more important near the sediment-water interface than it is deeper in the sediments and the reverse will hold for advective flux. In Eastern Brook Lake near the sediment-water interface, representative concentration gradients for HCO_3^-, Ca^{2+}, and Na^+ are 20, 4.5 and 1.7 μM/cm. Representative concentrations are 280, 115 and 40 μM. Using TD=0.5cm^{2}day^{-1} and v=0.0003 cm/day, the three ratios are 0.008, 0.015, and 0.014. Thus, advective flux due to sedimentation represents 1%-2% of diffusive flux at the sediment-water interface. At the largest value at which v had no visible effect on the modeled profiles, v=0.001cm/day, the three ratios as percents are 3%-5%, which is surprisingly high considering that the profiles are not visibly affected. At v=0.01cm/day, the ratios increase to 30%-50%. If the advection is downward (i.e., the lake leaks out the bottom), then this effect decreases the flux of most species, because the advective flux is opposite to the diffusive flux. It also decreases the diffusive flux by decreasing the gradient at the sediment-water interface, although this change is a smaller effect. Upward advection would increase the flux of most species, because the advective flux is is in the same direction as diffusive flux. If the upward advection were large enough, it would also increase

the diffusive flux by increasing the gradient at the sediment-water interface.

4.1.5. Adjustments for in-situ concentration and complex formation

Samples for analysis by atomic absorption spectrophotometry were transferred into acidified bottles, which prevented the precipitation of $Fe(OH)_3(s)$ after the oxidation of ferrous iron. Samples for alkalinity and gas measurements, however, were collected in unacidified containers, and the measurements were made after ferrous iron oxidized, forming a visible red precipitate. This reaction can be summarized as follows:

$$4Fe^{2+} + O_2 + 8HCO_3^- + 2H_2O = 4Fe(OH)_3(s) + 8CO_2$$

Hence, in-situ alkalinity should be greater and in-situ carbon dioxide should be less than measured, although the in-situ total of carbonate species should be the same as measured. The correctness of this scheme is reflected in the good charge balance we get by boosting in-situ alkalinity by ferrous charge equivalents. However, the symmetrical subtraction from carbon dioxide sometimes produces concentrations less than zero. This is probably because the gases were collected into evacuated containers, which limited the amount of oxygen available. Hence we have assumed that in-situ carbon dioxide is the same as measured.

The application of a similar scheme to manganese is more problematical, because its abiotic rate of oxidation is much slower than that of iron (Stumm and Morgan 1981, p. 466), and

hence it is uncertain how complete the oxidation was at the time of alkalinity titration and gas analysis. Ignoring this adjustment for manganese is also justified by its relatively low concentration.

In addition to the gross effects of oxidation after sampling, the formation of soluble complexes also influences molecular diffusion. The results of metal analysis by atomic absorption spectrophotometry are elemental totals, with no discrimination between complexes. Soluble complexes have different diffusion coefficients and charges from the complexing species, thus affecting diffusion rates, coulomb forces, and activity coefficient gradients. GEOCHEM (Sposito and Mattigod 1979), an equilibrium model designed for soil solutions, which includes all the metals and ligands of importance in the system of this study, was applied to determine which inorganic complexes were important in the system. The only species whose complexes amounted to more than five percent of their totals were iron and manganese.

Based on the species determined to be important, a simple equilibrium model was constructed following the method of Morel and Morgan (1972) for incorporation into the flux calculation program. Table 2 shows the modeled reactions together with the equilibrium constants and molar enthalpy changes. The constants for bicarbonate, carbonic acid, and water were temperature-corrected by empirical expressions. Other constants were temperature corrected using molar enthalpy changes. The model converts thermodynamic equilibrium constants to conditional constants using activity coefficients calculated from the Guntelberg

Table 2. Speciation: major reactions modeled in porewater			
Reaction	Equilibrium expression	Equilibrium constant (log K, 25°C) (ionic str.=0)	ΔH (kcal/mol)
$Fe^{2+}+CO_3^{2-}=FeCO_3^0$	$\frac{(FeCO_3^0)}{(Fe^{2+})(CO_3^{2-})}$	5.30[a]	3.[e]
$Fe^{2+}+H^+ +CO_3^{2-}=FeCO_3^0$	$\frac{(FeCO_3^0)}{(Fe^{2+})(H^+)(CO_3^{2-})}$	13.00[a]	-2.5[f]
$Mn^{2+}+CO_3^{2-}=MnCO_3^0$	$\frac{(MnCO_3^0)}{(Mn^{2+})(CO_3^{2-})}$	4.50[a]	3.[e]
$Mn^{2+}+H^+ +CO_3^{2-}=MnCO_3^0$	$\frac{(MnCO_3^0)}{(Mn^{2+})(H^+)(CO_3^{2-})}$	12.30[a]	-2.5[g]
$H^+ +CO_3^{2-}=HCO_3^-$	$\frac{(HCO_3^-)}{(H^+)(CO_3^{2-})}$	10.3[b]	-3.5[h]
$2H^+ +CO_3^{2-}=H_2CO_3^*$	$\frac{(H_2CO_3^*)}{(H^+)^2(CO_3^{2-})}$	16.7[c]	-5.5[h]
$H_2O=H^+ +OH^-$	$(H^+)(OH^-)$	-14.00[d]	

Notes:

$H_2CO_3^* = H_2CO_3+CO_2(aq)$

a. Sposito and Mattigod (1979)

b. Stumm and Morgan (1981), p. 206. Temperature corrections are based on an equation fitted to the empirical data in this reference:
log K = -6.529+2906./T+0.02385*T, where T is temperature in Kelvins

c. Stumm and Morgan (1981), pp. 205 and 206. Temperature corrections are based on an equation fitted to the empirical data in this reference:
log K = -21.35+6307./T+0.0566*T, where T is temperature in Kelvins

d. Stumm and Morgan (1981), p. 126. Temperature corrections are based on an equation fitted to the empirical data in this reference:
log K = 3.483-4077./T-0.01276*T, where T is temperature in Kelvins

e. Crude estimate based on Ca^{2+} and Mg^{2+}, Martell and Smith (1982), p. 403. The sign, at least, is probably correct.

f. Crude estimate, based on Mn^{2+}, Smith and Martell (1976), p. 403. The sign is probably correct.

g. Crude estimate, Martell and Smith (1982), p. 403. The sign is probably correct.

h. Smith and Martell (1976), p. 37.

approximation.[8] Inputs to the model were total iron, total manganese, total carbonate species, and in-situ alkalinity. Using the equilibrium expressions, all unknown species were written in terms of four unknowns: H^+, Mn^{2+}, Fe^{2+}, and CO_3^{2-}. These allowed four equations to be written: mass balances for manganese, iron, and carbonate species, and charge balance. These four non-linear algebraic equations were solved using a standard multi-dimensional Newton-Raphson algorithm (Press et al. 1986), which was then iterated until ionic strength converged.

4.2. Calculations of fluxes from peeper data

4.2.1. Introduction

To do these calculations, the following data are needed: temperature, concentrations, concentration gradients, velocities, diffusion coefficients, porosity, and tortuosity. Concentrations, gradients, porosity, temperature, and the velocity resulting from deposition have been measured. Molecular diffusion coefficients and tortuosity were estimated as described above. However, certain fluxes cannot be easily calculated by these methods. The most important of these is the eddy-diffusive flux resulting from a gradient too small for the precision of gradient measurements. This flux could be quite large if the eddy-diffusion coefficient is large. In the system of this study,

[8] The Guntelberg approximation for activity coefficients is (Stumm and Morgan 1981, p. 135): $\log \gamma_i = -0.5 z_i^2 \frac{\sqrt{I}}{1+\sqrt{I}}$

such a situation is likely to exist at the sediment-water interface. High rates of organic matter decomposition take place under aerobic conditions, but the transport of products into the overlying water is so rapid that concentration gradients large enough to measure do not develop. Of course, if these gradients were measurable, we would still have to find methods of measuring or estimating the eddy diffusion coefficients. Such methods are much more poorly developed for eddy diffusion than for molecular diffusion. Hence, the gradient-based calculations presented here are limited to species generated in regions where molecular diffusion dominates transport. Such regions are usually within the sediments, but may include the interface region and some overlying water during the under-ice periods when the bottom waters are very still.

If the location of the sediment-water interface is known exactly, from direct observation, a gradient can be estimated between the sediment-water interface and the first peeper chamber below the sediment-water interface by assuming that the concentration at the sediment-water interface is the same as in the overlying water. If there is a boundary layer, however, slow transport will result in a higher concentration at the sediment-water interface than in the overlying water, and therefore the use of a gradient that is too high. Nonetheless, this procedure is probably one of the best methods of calculating fluxes from observed gradients, but it is not one we can use, because we do not have direct observation of the sediment-water interface.[9]

[9] While the sediment-water interface is known approximately from sharp profile changes, the certainty is no better than the closest spacing of the peeper chambers: roughly 3cm for the short

The concentration in a peeper chamber centered at the sediment-water interface is not a good estimate of the concentration at the sediment-water interface, because of the vertical span of a single peeper chamber and because the gradient is especially variable at the sediment-water interface. At greater depths in the sediment, where the gradient may be approximated as constant over the vertical span of a peeper chamber, the concentration in the chamber is a good estimate of the porewater concentration at the center of the chamber.

The approach used here is to take a measured gradient at some point within the sediments, but close to the sediment-water interface. The concentrations in the peeper chambers are then reasonable estimates of the concentrations of porewater at the centers of the chambers, and the distance between the centers of the chambers is known precisely. The gradient calculated from these concentrations and this distance is then used to calculate the flux across some specified flux plane, somewhere between the two peeper chambers, by using the porosity, tortuosity, and concentration[10] at the flux plane. Since fluxes across the sediment-water interface are of interest, some calculations have

---

peepers and 10cm for the long peepers. Since the distance from the sediment-water interface to the first peeper below the sediment-water interface would be the denominator of a gradient estimation, this method would be highly uncertain.

[10] Concentration must be taken into account because the activity coefficient varies nonlinearly with ionic strength and because the electrical correction is apportioned among the diffusing ions according to their concentration. For the same concentration gradient, $\nabla\gamma_i$ will be larger nearer the sediment-water interface where the ionic strength is low. This can be seen mathematically by starting from the Guntelberg approximation and observing that $d\gamma/dI<0$ and $d^2\gamma/dI^2>0$.

been made using the sediment-water interface as the flux plane, while using a gradient measured somewhat below the sediment-water interface. At the sediment-water interface, porosity is estimated by extrapolation, tortuosity is estimated from porosity, and concentration is taken to be that of the overlying water. The assumption inherent in this approach is that the gradient measured somewhat below the sediment-water interface is the same as the gradient at the sediment-water interface. The result is less defensible than using a flux plane between the peeper chambers used to calculate the gradient, but the exercise illustrates some important effects that concentrations at the flux plane have on fluxes.

4.2.2. Methods

In order to explore the effects of flux plane concentrations, activity coefficients, coulomb forces, and complex formation on fluxes, 24 methods were used to calculate the fluxes for each peeper. The methods were combinations generated by a 2×2×2×3 tree. The first three levels (2×2×2) generated 8 sets of concentrations at a flux plane and a "dummy plane" (0.01cm below the flux plane). The "dummy plane" is simply a plane chosen close to the flux plane for the purposes of gradient calculation. It needs to be close so that the activity coefficient gradients are accurate. The fourth level consisted of three methods of flux calculations for each set of flux and dummy plane concentrations.

Level 1: Flux plane

(1)

Specify a depth for the flux plane and interpolate between peeper chambers to generate concentrations at the flux and dummy planes.

(2)

Specify a concentration (such as the overlying water) for the flux plane, and then use the measured gradients to extrapolate to the dummy plane. The purpose of specifying a concentration for the flux plane was to explore the effects of concentration at the flux plane while keeping the gradients constant.

Level 2: Charge balance

(1)

Keep concentrations as generated in Level 1.

(2)

Adjust the concentrations generated in Level 1 to produce charge balance. This adjustment was done by increasing or decreasing the concentration of each species in proportion to its concentration and charge. The purpose of the charge balance adjustment was to be able to separate the effects of initial charge imbalance from charge imbalance caused by differential diffusion.

Level 3: Speciation

(1)

Keep concentrations as generated in Level 2

(2)

Calculate the concentrations of various complexes using the equilibrium program described previously.

At the conclusion of this level, there were then 8 sets of flux and dummy plane concentrations. For each of these, a concentration gradient was calculated between the flux and dummy planes. For each of these 8 sets of concentrations and gradients, fluxes were calculated in the following three ways:

Level 4: Flux calculation method

(1)

Fluxes were calculated using the concentration gradients:

$$J = -\phi TD_i \frac{\partial C_i}{\partial x}$$

(2)

Fluxes were calculated adjusting the concentration gradients for activity coefficients:

$$J = -\phi TD_i \left(\frac{C_i}{\gamma_i} \frac{\partial \gamma_i}{\partial x} + \frac{\partial C_i}{\partial x} \right)$$

(3)

Fluxes were calculated using the adjusted gradients in (2) with an electrical correction to assure a charge-balanced flux:

$$J = -\phi TD_i \left(\frac{C_i}{\gamma_i} \frac{\partial \gamma_i}{\partial x} + \frac{\partial C_i}{\partial x} \right) + \frac{\phi TD_i z_i C_i}{\sum_{j=1}^{n} z_j^2 C_j D_j} \sum_{k=1}^{n} z_k D_k \left(\frac{C_k}{\gamma_k} \frac{\partial \gamma_k}{\partial x} + \frac{\partial C_k}{\partial x} \right)$$

In each case, concentrations at the flux and dummy planes (0.01cm apart) were used to estimate the gradients, and

concentrations were those at the flux plane.

4.2.3. Results: discussion of various factors

To examine the importance of the various factors affecting molecular diffusive fluxes (activity coefficient gradients, coulomb forces, and complex formation), the calcium fluxes resulting from the different combinations of flux plane, charge balance, speciation, and calculational method are presented for the six long peepers in Table 3.

The effect of activity coefficient gradients is to decrease the flux of species diffusing out of the sediments. The percentage change in flux resulting from applying the correction for activity coefficient, PC12, is thus always negative, since the ionic-strength gradient has the same sign as the calcium concentration gradient, and therefore the activity coefficient gradient has the opposite sign from the calcium concentration gradient.

The activity correction produces a flux decrease of 0.331nmol $cm^{-2}day^{-1}$ (-19%) in EBLPB and 0.400nmol $cm^{-2}day^{-1}$ (-14%) in EBLPR. This correction is the product of three factors (see equation 16). The first is the activity coefficient gradient. The activity coefficient gradient for EBLPB is -0.0052, while that for EBLPR is -0.0076. The second factor is the concentration of calcium, 135μM for EBLPB and 110μM for EBLPR. The third factor is the inverse of the activity coefficient, which is 1/0.82 for EBLPB and 1/0.86 for EBLPR. The first factor is the dominant difference, thus resulting in the larger correction for EBLPR, although the second and third factors have the opposite

Table 3. Six long peepers: 24 calcium fluxes

Flux plane	Charge bal.	Peeper	Fluxes									
			Unspeciated					Speciated				
			FLX1	FLX2	PC12	FLX3	PC23	FLX1	FLX2	PC12	FLX3	PC23
I	NA	EBLPB	-1.747	-1.416	-18.9	-2.267	60.1	-1.747	-1.480	-15.3	-2.071	39.9
		EBLPR	-2.791	-2.391	-14.3	-3.331	39.3	-2.791	-2.442	-12.5	-3.092	26.6
		EMLPB	-0.947	-0.872	-8.0	-1.017	16.7	-0.947	-0.884	-6.6	-0.969	9.5
		EMLPR	-0.284	-0.252	-11.3	-0.303	20.0	-0.284	-0.256	-10.1	-0.284	11.2
		MOLPB	-1.965	-1.911	-2.8	-1.909	-0.1	-1.965	-1.915	-2.5	-1.873	-2.2
		MOLPR	-2.254	-2.095	-7.0	-2.563	22.3	-2.254	-2.113	-6.3	-2.477	17.2
	A	EBLPB	-1.780	-1.460	-17.9	-2.321	58.9	-1.780	-1.522	-14.5	-2.140	40.6
		EBLPR	-2.654	-2.279	-14.1	-3.594	57.7	-2.654	-2.327	-12.3	-3.402	46.2
		EMLPB	-0.921	-0.847	-8.1	-1.030	21.6	-0.921	-0.860	-6.7	-0.987	14.8
		EMLPR	-0.296	-0.263	-11.0	-0.292	10.9	-0.296	-0.267	-9.9	-0.272	1.8
		MOLPB	-1.897	-1.844	-2.8	-1.948	5.6	-1.897	-1.849	-2.6	-1.921	3.9
		MOLPR	-2.228	-2.076	-6.8	-2.567	23.6	-2.228	-2.093	-6.1	-2.489	18.9
S	NA	EBLPB	-1.979	-1.382	-30.2	-4.859	251.5	-1.979	-1.402	-29.2	-4.769	240.1
		EBLPR	-2.969	-2.605	-12.3	-4.135	58.7	-2.969	-2.617	-11.8	-4.058	55.0
		EMLPB	-1.322	-1.215	-8.1	-2.059	69.4	-1.322	-1.219	-7.8	-2.921	139.6
		EMLPR	-0.383	-0.342	-10.7	-0.593	73.3	-0.383	-0.343	-10.6	-0.658	92.1
		MOLPB	-2.296	-2.261	-1.5	-2.237	-1.1	-2.296	-2.262	-1.5	-2.221	-1.8
		MOLPR	-2.551	-2.297	-10.0	-4.023	75.2	-2.551	-2.302	-9.8	-3.905	69.7
	A	EBLPB	-3.997	-3.505	-12.3	-6.334	80.7	-3.997	-3.522	-11.9	-6.219	76.6
		EBLPR	-1.521	-1.130	-25.7	-3.869	242.4	-1.521	-1.143	-24.8	-3.797	232.1
		EMLPB	-1.692	-1.600	-5.4	-2.445	52.8	-1.692	-1.603	-5.3	-3.022	88.6
		EMLPR	-0.625	-0.587	-6.1	-0.733	24.9	-0.625	-0.587	-6.0	-0.765	30.1
		MOLPB	-2.141	-2.108	-1.5	-2.282	8.3	-2.141	-2.109	-1.5	-2.266	7.5
		MOLPR	-3.607	-3.409	-5.5	-4.828	41.6	-3.607	-3.412	-5.4	-4.718	38.3

Notes:

Flux plane: I = concentrations interpolated, S = concentrations specified

Charge balance: N = not adjusted, A = adjusted

FLX1,FLX2,FLX3: Flux calculation method as described under Level 4 in the text

Flux units are nmol $cm^{-2}day^{-1}$

PC12: Percentage change between FLX1 and FLX2, =100(FLX2-FLX1)/FLX1

PC23: Percentage change between FLX2 and FLX3, =100(FLX3-FLX2)/FLX2

effect. The percent change in EBLPB is greater because the uncorrected flux is smaller.

In the Emerald Lake long peepers, the activity correction produces a flux decrease of 0.075nmol $cm^{-2}day^{-1}$ (-8%) in EMLPB and 0.032nmol $cm^{-2}day^{-1}$ (-11%) in EMLPR. The three factors for each peeper are $-0.0066cm^{-1}$, 33.00μM, and 1/.83; and $-0.0036cm^{-1}$, 25.25μM, and 1/.87. In this case, all three factors are strongest for EMLPB, as is reflected in the greater absolute change in flux. The percent change in EMLPR is greater because the uncorrected flux is smaller.

The sign of the electrical correction (as a percentage, PC23 in Table 3) depends on whether iron or ammonium is the major positive diffusing species. Excess positive charge will tend to accumulate if ammonium is the major diffusing species (i.e., has the highest concentration gradient), because ammonium has a higher diffusion coefficient than bicarbonate, the major negative species. Excess negative charge will tend to accumulate if iron is the major diffusing species, because iron has a lower diffusion coefficient than bicarbonate. Three examples are shown in Table 4. Since the examples used are for concentrations that are not charge balanced, there is some question as to whether a flux charge imbalance is the result of differential diffusion or simply poor initial charge balance. Comparison of the "charge balance not adjusted" (NA) and "charge balance adjusted" (A) calculations in Table 3 indicates that the basic effect remains the same.

Table 4. Factors affecting electrical corrections: three examples (flux plane concentrations interpolated, charge balance not adjusted)

Parameter	Peeper		
	EBLPB	MOLPB	MOLPR
Charge imbalance resulting from the flux (neq $cm^{-2}day^{-1}$)	14.	-0.66	8.7
% effect on Ca flux	60.%	-0.1%	22.%
∇Ca^{2+}(nmol cm^{-4})	3.6	4.9	5.2
∇Fe^{2+}(nmol cm^{-4})	34.	10.5	22.
∇NH_4^+(nmol cm^{-4})	9.	10.	9.
$[Ca^{2+}](\mu M)$	135.	30.	55.
$[Fe^{2+}](\mu M)$	500.	220.	234.
$[NH_4^+](\mu M)$	104.	63.	58.4

The size of the electrical correction to the calcium fluxes also depends on the concentration of positive species at the flux plane, as well as the size of the imbalance. If there is a lot of ammonium and iron at the flux plane, these species will carry the bulk of the correction. If they are of relatively low concentration compared with calcium, as they are likely to be at the sediment-water interface, then calcium will carry most of the correction. An example is EBLPB with specified (sediment-water interface) flux-plane concentrations (see Table 3). In this case, calcium flux is more than doubled by the electrical correction. Thus, while the charge imbalance is generated by species with high *gradients*, the correction affects species with high *concentrations*. In Table 3, the specified flux-plane concentration is an estimate of the sediment-water interface concentration. At this location, calcium tends to be the important positive ion, and it is apparent that the effect of the electrical correction on calcium flux is usually much greater than for the case where the flux-plane concentrations were interpolated.

One effect of complex formation is to decrease the activity correction. This occurs because complex formation reduces ionic strength to a larger extent where concentrations are higher. Hence, activity-coefficient gradients are reduced. The effect of complex formation on the electrical correction can go either way. In some cases, the charge imbalance is reduced because the gradients of charged species are reduced. In other cases, the effect of the correction on calcium is enhanced because the concentration of other positively charged species is reduced.

In conclusion, all three of the effects examined (activity coefficient gradients, coulomb forces, and complex formation) can have a significant effect on molecular-diffusive fluxes. The dramatic differences in electrical effects between the fluxes of the interpolated case (within sediment) and specified case (at the sediment-water interface) suggest that extrapolating measured gradients to the sediment-water interface is not a good idea. The use of charge-balanced concentrations at the flux and dummy planes was primarily a device for examining the electrical correction, and has no direct justification in doing actual flux calculations. Hence, the procedure followed in the following calculations uses gradients generated from interpolated, speciated flux- and dummy-plane concentrations, with both activity and electrical corrections.

4.2.4. Results: three lakes summer peepers

Calculations were done for summer peepers for which the aluminum plate was above the sediment-water interface. If the plate was at or below the sediment-water interface, it acted as an impermeable barrier that distorted the natural fluxes. Because of the softness and depth of the Eastern Brook Lake sediments, all of the summer short peepers got buried, and only the winter peepers and long peepers provided acceptable data.

Flux calculations for the three lakes were done by selecting representative pairs of peeper chambers near, but not at or above, the sediment-water interface. The chambers representing the steepest gradient were chosen, but obvious outliers were

avoided. For the short peepers, because all species were not analyzed in all chambers, the pairs of chambers were different for different species. A flux plane roughly central to the groups of chambers was chosen. The dummy plane was always 0.01cm below the flux plane. The concentrations at the flux and dummy planes were calculated by interpolation and then speciated independently. The charge balance at the flux planes, an indicator of the quality of the analysis and the legitimacy of the interpolation procedure, is listed at the bottom of Tables 5, 6, and 7. Concentration gradients were calculated using the concentrations at the flux and dummy planes. Fluxes were then calculated using both activity and electrical corrections. The fluxes of individual species are presented in Tables 5, 6, and 7, in order of decreasing mean flux.

The fluxes of elemental and some other totals are presented in Tables 8, 9, and 10, in order of decreasing mean flux. The fluxes in all three lakes were dominated by carbon, followed by the trio of silica, nitrogen and iron (not necessarily in that order), followed by the base cations (calcium, magnesium, sodium and potassium). Standard deviations of fluxes for elemental totals based on replicate peepers are presented in Table 11.

4.3. Discussion

Table 5. Eastern Brook Peeper Fluxes (nmol $cm^{-2}day^{-1}$): Species
(Flux-plane concentrations interpolated and speciated, charge balance not adjusted, activity and electrical corrections applied)

Species	Peeper (date: YYMMDD)				
	EBLPB (860729)	EBLPR (860729)	*n*	mean	sd
HCO3	-39.925	-43.930	2	-41.928	2.833
CO2	-36.040	-35.770	2	-35.905	0.193
CH4	-28.652	-16.737	2	-22.695	8.425
SIO2	-17.096	-11.107	2	-14.101	4.235
NH4	-9.717	-10.441	2	-10.079	0.512
FE	-8.289	-10.118	2	-9.204	1.294
FEHCO3	-6.564	-4.228	2	-5.396	1.652
CA	-2.088	-3.117	2	-2.602	0.728
NA	-1.298	-0.796	2	-1.047	0.354
K	-0.978	-0.986	2	-0.982	0.006
MG	-0.252	-0.467	2	-0.359	0.152
FECO3	-0.356	-0.237	2	-0.296	0.085
CL	-0.042	-0.073	2	-0.057	0.022
SO4	0.034	0.031	2	0.033	0.002
MN	-0.006	-0.045	2	-0.025	0.028
NO2	0.054	-0.018	2	0.018	0.051
MNHCO3	-0.012	-0.017	2	-0.015	0.003
NO3	0.005	0.023	2	0.014	0.012
BR	.	-0.013	1	-0.013	.
CO3	-0.005	-0.006	2	-0.006	0.001
H	-0.009	-0.001	2	-0.005	0.006
MNCO3	0.000	-0.001	2	-0.001	0.000
OH	0.000	0.000	2	0.000	0.000
Charge balance:					
COA	1.094	1.132	2	1.113	0.027
CMA	115.880	89.145	2	102.513	18.905

Notes:
A dot indicates a missing value
COA= cations over anions for concentrations at the flux plane
CMA= cations minus anions for concentrations at the flux plane

Table 6. Emerald Lake Peeper Fluxes (nmol $cm^{-2}day^{-1}$): Species
(Flux-plane concentrations interpolated and speciated, charge balance not adjusted, activity and electrical corrections applied)

Species	Peeper (date: YYMMDD)								
	EMLPB (860819)	EMLPR (860819)	EMP3B (850905)	EMP3R (850905)	EMP4B (851002)	EMP4R (851002)	*n*	mean	sd
CO2	-42.329	-47.295	.	.	-119.974	-90.341	4	-74.985	36.937
CH4	-37.587	-24.773	.	.	-85.728	-61.264	4	-52.338	26.907
HCO3	-34.545	-18.136	-20.646	-15.230	-38.259	-76.958	6	-33.962	23.005
SIO2	-8.785	-10.306	-32.817	-22.456	-49.863	-29.589	6	-25.636	15.383
NH4	-10.962	-9.179	-16.837	-10.356	-16.091	-35.236	6	-16.444	9.729
FE	-6.890	-2.282	-0.025	-1.312	-6.167	-12.616	6	-4.882	4.660
FEHCO3	-5.054	-1.276	-0.140	-0.172	-1.497	-6.493	6	-2.439	2.681
NA	-1.568	-1.384	-2.005	-1.552	-2.007	-2.989	6	-1.917	0.584
CA	-0.973	-0.286	-0.647	-0.305	-2.089	-2.668	6	-1.161	0.993
K	-0.642	-0.462	-0.435	-0.247	-1.399	-0.814	6	-0.666	0.407
MG	-0.365	-0.169	0.004	-0.045	-0.226	-0.308	6	-0.185	0.145
FECO3	-0.172	-0.024	0.194	-0.202	-0.025	-0.162	6	-0.065	0.148
MN	-0.015	-0.121	-0.031	-0.002	-0.048	-0.132	6	-0.058	0.055
NO2	.	-0.016	-0.091	-0.043	0.015	.	4	-0.034	0.045
CL	-0.071	-0.009	-0.057	-0.075	.	0.056	5	-0.031	0.056
BR	-0.010	-0.001	.	-0.076	.	.	3	-0.029	0.041
NO3	-0.001	0.002	-0.091	-0.071	0.007	0.005	6	-0.025	0.044
H	0.008	-0.027	0.000	-0.001	-0.108	0.200	6	0.012	0.101
MNHCO3	-0.008	-0.009	-0.001	-0.001	-0.005	-0.011	6	-0.006	0.004
OH	0.000	0.000	0.002	0.024	0.000	-0.001	6	0.004	0.010
CO3	-0.003	-0.001	0.072	-0.038	-0.001	-0.006	6	0.004	0.036
SO4	-0.039	0.054	-0.037	-0.057	0.037	0.060	6	0.003	0.053
MNCO3	0.000	0.000	0.001	-0.001	0.000	0.000	6	0.000	0.001
Charge balance:									
COA	1.026	0.981	1.011	0.965	0.979	0.979	6	0.990	0.023
CMA	28.469	-13.480	3.261	-6.402	-7.328	-14.875	6	-1.726	16.130

Notes:
A dot indicates a missing value
COA= cations over anions for concentrations at the flux plane
CMA= cations minus anions for concentrations at the flux plane

Table 7. Mosquito Lake Peeper Fluxes (nmol $cm^{-2}day^{-1}$): Species
(Flux-plane concentrations interpolated and speciated, charge balance not adjusted, activity and electrical corrections applied)

Species	Peeper (date: YYMMDD)									
	MOLPB (860924)	MOLPR (860924)	MOP2R (850716)	MOP3B (850808)	MOP3R (850808)	MOP4B (850917)	MOP4R (850917)	*n*	mean	sd
CO2	-37.127	-50.183	-45.131	-20.793	-118.938	-119.610	-82.871	7	-67.808	39.794
HCO3	-22.697	-35.055	-22.632	-64.837	-92.024	-43.503	-111.686	7	-56.062	34.867
CH4	-7.394	-21.944	-26.714	-21.566	-89.141	-69.514	-57.881	7	-42.022	30.228
SIO2	-14.428	-16.145	.	-19.615	-23.764	-25.698	-28.035	6	-21.281	5.430
NH4	-9.854	-9.922	-16.370	-24.078	-18.383	-19.334	-20.805	7	-16.964	5.377
FE	-2.294	-6.833	-0.807	-10.893	-24.293	-1.260	-28.029	7	-10.630	11.237
FEHCO3	-1.448	-3.024	-0.152	-6.959	-12.090	-0.293	-5.972	7	-4.277	4.351
CA	-1.877	-2.486	-1.338	-2.315	-3.430	-7.174	-5.817	7	-3.491	2.184
FECO3	-0.042	-0.104	-0.003	-0.514	-0.226	-0.003	20.657	7	2.823	7.866
NA	-1.206	-1.630	-1.618	-2.737	-2.205	-1.113	-2.838	7	-1.907	0.698
MG	-0.811	-0.672	-0.110	-1.346	-0.905	-2.874	-1.060	7	-1.111	0.865
K	-0.672	-0.649	0.025	-1.746	-1.272	-0.716	-1.337	7	-0.909	0.584
CO3	-0.002	-0.003	-0.001	-0.016	0.022	-0.001	3.579	7	0.511	1.353
OH	0.000	0.000	0.000	-0.002	0.016	0.000	2.689	7	0.386	1.016
NO2	0.048	.	.	0.028	0.113	.	.	3	0.063	0.044
SO4	-0.091	-0.033	0.021	0.053	0.036	0.052	0.287	7	0.046	0.118
H	-0.021	-0.023	0.056	0.059	-0.158	0.691	-0.316	7	0.041	0.316
CL	-0.350	-0.107	0.025	0.147	0.315	0.004	0.126	7	0.023	0.211
NO3	0.001	0.011	0.002	0.014	0.037	0.004	0.060	7	0.019	0.022
BR	.	-0.018	.	.	.	.	.	1	-0.018	.
MN	-0.007	-0.005	0.002	-0.002	-0.028	-0.006	.	6	-0.007	0.010
MNHCO3	-0.004	-0.003	-0.001	-0.003	-0.009	-0.002	.	6	-0.004	0.003
MNCO3	0.000	0.000	0.000	0.000	0.000	0.000	.	6	0.000	0.000
Charge balance:										
COA	0.998	1.108	0.721	0.984	0.995	0.980	0.906	7	0.956	0.119
CMA	-1.331	64.374	-92.685	-14.145	-4.331	-5.034	-37.012	7	-12.881	46.885

Notes:
A dot indicates a missing value
COA= cations over anions for concentrations at the flux plane
CMA= cations minus anions for concentrations at the flux plane

Table 8. Eastern Brook Peeper Fluxes (nmol $cm^{-2}day^{-1}$): Elemental Totals (Flux-plane concentrations interpolated and speciated, charge balance not adjusted, activity and electrical corrections applied)

Species	Peeper (date: YYMMDD)				
	EBLPB (860729)	EBLPR (860729)	*n*	mean	sd
CCT	-111.555	-100.926	2	-106.240	7.516
FET	-15.209	-14.583	2	-14.896	0.443
SIO2	-17.096	-11.107	2	-14.101	4.235
NT	-9.657	-10.437	2	-10.047	0.551
CA	-2.088	-3.117	2	-2.602	0.728
NA	-1.298	-0.796	2	-1.047	0.354
K	-0.978	-0.986	2	-0.982	0.006
MG	-0.252	-0.467	2	-0.359	0.152
CL	-0.042	-0.073	2	-0.057	0.022
MNT	-0.018	-0.063	2	-0.041	0.032
SO4	0.034	0.031	2	0.033	0.002
BR	.	-0.013	1	-0.013	.
Other totals:					
CO3T	-46.863	-48.419	2	-47.641	1.100
CT	-82.902	-84.189	2	-83.546	0.908
SBC	-6.956	-8.949	2	-7.953	1.410

Notes:
A dot indicates a missing value
FET=FE+FEHCO3+FECO3
MNT=MN+MNHCO3+MNCO3
NT=NH4+NO3+NO2
CO3T=HCO3+CO3+FEHCO3+FECO3+MNHCO3+MNCO3
CT=CO3T+CO2
CCT=CT+CH4 (total carbon)
SBC=2*CA+2*MG+NA+K (sum of base cations) (neq $cm^{-2}day^{-1}$)

Table 9. Emerald Lake Peeper Fluxes (nmol $cm^{-2}day^{-1}$): Elemental Totals
(Flux-plane concentrations interpolated and speciated, charge balance not adjusted, activity and electrical corrections applied)

Species	Peeper (date: YYMMDD)								
	EMLPB (860819)	EMLPR (860819)	EMP3B (850905)	EMP3R (850905)	EMP4B (851002)	EMP4R (851002)	*n*	mean	sd
CCT	-119.698	-91.514	.	.	-245.490	-235.235	4	-172.984	78.759
SIO2	-8.785	-10.306	-32.817	-22.456	-49.863	-29.589	6	-25.636	15.383
NT	-10.963	-9.194	-17.019	-10.470	-16.069	-35.231	6	-16.491	9.713
FET	-12.116	-3.583	0.030	-1.686	-7.688	-19.271	6	-7.386	7.289
NA	-1.568	-1.384	-2.005	-1.552	-2.007	-2.989	6	-1.917	0.584
CA	-0.973	-0.286	-0.647	-0.305	-2.089	-2.668	6	-1.161	0.993
K	-0.642	-0.462	-0.435	-0.247	-1.399	-0.814	6	-0.666	0.407
MG	-0.365	-0.169	0.004	-0.045	-0.226	-0.308	6	-0.185	0.145
MNT	-0.023	-0.130	-0.031	-0.004	-0.053	-0.143	6	-0.064	0.058
CL	-0.071	-0.009	-0.057	-0.075	.	0.056	5	-0.031	0.056
BR	-0.010	-0.001	.	-0.076	.	.	3	-0.029	0.041
SO4	-0.039	0.054	-0.037	-0.057	0.037	0.060	6	0.003	0.053
Other totals:									
CO3T	-39.783	-19.446	.	.	-39.787	-83.630	4	-45.661	27.067
CT	-82.111	-66.740	.	.	-159.762	-173.971	4	-120.646	54.050
SBC	-4.886	-2.757	-3.725	-2.500	-8.036	-9.754	6	-5.276	2.976

Notes:
A dot indicates a missing value
FET=FE+FEHCO3+FECO3
MNT=MN+MNHCO3+MNCO3
NT=NH4+NO3+NO2
CO3T=HCO3+CO3+FEHCO3+FECO3+MNHCO3+MNCO3
CT=CO3T+CO2
CCT=CT+CH4 (total carbon)
SBC=2*CA+2*MG+NA+K (sum of base cations) (neq $cm^{-2}day^{-1}$)

Table 10. Mosquito Lake Peeper Fluxes (nmol $cm^{-2}day^{-1}$): Elemental Totals (Flux-plane concentrations interpolated and speciated, charge balance not adjusted, activity and electrical corrections applied)

Species	Peeper (date: YYMMDD)									
	MOLPB (860924)	MOLPR (860924)	MOP2R (850716)	MOP3B (850808)	MOP3R (850808)	MOP4B (850917)	MOP4R (850917)	*n*	mean	sd
CCT	-68.713	-110.317	-94.635	-114.688	-312.406	-232.927	-234.175	7	-166.837	92.058
SIO2	-14.428	-16.145	.	-19.615	-23.764	-25.698	-28.035	6	-21.281	5.430
NT	-9.805	-9.911	-16.368	-24.036	-18.233	-19.330	-20.745	7	-16.918	5.367
FET	-3.785	-9.961	-0.962	-18.366	-36.609	-1.556	-13.344	7	-12.083	12.586
CA	-1.877	-2.486	-1.338	-2.315	-3.430	-7.174	-5.817	7	-3.491	2.184
NA	-1.206	-1.630	-1.618	-2.737	-2.205	-1.113	-2.838	7	-1.907	0.698
MG	-0.811	-0.672	-0.110	-1.346	-0.905	-2.874	-1.060	7	-1.111	0.865
K	-0.672	-0.649	0.025	-1.746	-1.272	-0.716	-1.337	7	-0.909	0.584
SO4	-0.091	-0.033	0.021	0.053	0.036	0.052	0.287	7	0.046	0.118
CL	-0.350	-0.107	0.025	0.147	0.315	0.004	0.126	7	0.023	0.211
BR	.	-0.018	.	.	.	.	.	1	-0.018	.
MNT	-0.011	-0.008	0.001	-0.005	-0.037	-0.008	.	6	-0.011	0.013
Other totals:										
CO3T	-24.192	-38.189	-22.789	-72.329	-104.327	-43.803	-93.423	7	-57.007	33.107
CT	-61.319	-88.373	-67.920	-93.122	-223.265	-163.414	-176.294	7	-124.815	62.495
SBC	-7.254	-8.594	-4.490	-11.805	-12.147	-21.924	-17.929	7	-12.020	6.113

Notes:
A dot indicates a missing value
FET=FE+FEHCO3+FECO3
MNT=MN+MNHCO3+MNCO3
NT=NH4+NO3+NO2
CO3T=HCO3+CO3+FEHCO3+FECO3+MNHCO3+MNCO3
CT=CO3T+CO2
CCT=CT+CH4 (total carbon)
SBC=2*CA+2*MG+NA+K (sum of base cations) (neq $cm^{-2}day^{-1}$)

Table 11. Standard deviations of calculated elemental total fluxes based on pooled variances from replicate peepers from three lakes (nmol $cm^{-2}day^{-1}$, except SBC, which is neq $cm^{-2}day^{-1}$)

Species	Degrees of freedom	Standard deviation
BR	1	0.0064
CA	7	0.6233
CCT	6	59.0461
CL	6	0.0946
CO3T	6	22.3982
CT	6	39.0244
FET	7	7.1725
K	7	0.2700
MG	7	0.5070
MNT	6	0.0441
NA	7	0.5912
NT	7	5.6663
SBC	7	1.4839
SIO2	7	6.4486
SO4	7	0.0699
Other totals:		
CO3T	6	22.3982
CT	6	39.0244
SBC	7	1.4839

Notes:
A dot indicates a missing value
FET=FE+FEHCO3+FECO3
MNT=MN+MNHCO3+MNCO3
NT=NH4+NO3+NO2
CO3T=HCO3+CO3+FEHCO3+FECO3+MNHCO3+MNCO3
CT=CO3T+CO2
CCT=CT+CH4 (total carbon)
SBC=2*CA+2*MG+NA+K (sum of base cations) (neq $cm^{-2}day^{-1}$)

4.3.1. Origins of fluxes

Table 12 compares the gradient-calculated fluxes as mole percents of carbon with those assembled by Vallentyne (1974) as averages for freshwater flora. While Vallentyne's values can be considered only rough approximations to the elemental composition of the biota which form the sediments in the lakes of this study, the numbers are consistent with organic-matter decomposition being a source of the major species except iron. However, Vallentyne's analyses are of living plants, and, if many of the base cations are contained in the cytoplasm, cell lysis, which is likely to occur when the plants die, would release these base cations. Since the plants die before they are buried in the sediments, the sedimentary organic matter is likely to contain fewer base cations than Vallentyne's analysis would indicate. Nonetheless, some base cations are likely to be released from the decomposition of organic matter. An elemental analysis of the sedimentary organic matter in our lakes could resolve this question. The remaining base cations must be originating from mineral dissolution.

In an effort to examine the relationship of the fluxes to mineral weathering, we have used the mean water column concentrations of base cations as estimates of average mineral weathering in the watershed, including the minerals in the sediments. Table 13 compares the gradient-calculated fluxes as mole percents of calcium with both mean water column values and with those assembled by Vallentyne as averages for freshwater flora. This table suggests that sodium is likely to be primarily a product of

Table 12. Elemental fluxes for three lakes and the elemental composition freshwater flora (Vallentyne 1974) normalized as mole percents of carbon

Element	Mole-percent of carbon			
	Vallentyne (1974)	Eastern Brook	Emerald	Mosquito
Carbon	100.	100.	100.	100.
Silica	8.6	13.	21.	13.
Nitrogen	9.2	9.4	14.	10.
Calcium	1.8	2.4	0.96	2.1
Potassium	1.4	0.92	0.55	0.54
Magnesium	0.53	0.34	0.15	0.67
Sodium	0.32	1.0	1.6	1.1
Iron	0.07	14.	6.1	7.2

Table 13. Base cation fluxes for three lakes, the base cation composition freshwater flora (Vallentyne 1974), and the mean water column concentrations of base cations normalized as mole percents of calcium

Cation	Mole-percent of calcium						
	Vallentyne (1974)	Eastern Brook		Emerald		Mosquito	
		Flux	WC	Flux	WC	Flux	WC
Calcium	100	100	100	100	100	100	100
Magnesium	14	14	15	16	21	32	53
Sodium	9	40	68	165	146	55	130
Potassium	38	38	25	57	25	26	23

WC=water column

mineral weather rather than decomposition of organic matter. Magnesium and potassium could be either. A firm resolution of the origin of base cations will have to await further work. An analysis of the base cations in the sedimentary organic matter would be a good start.

4.3.2. Comparison of gradient-calculated fluxes with other measurements

Melack et al. (1987) measured fluxes using benthic chambers, mesocosm bags, and in-lake measurement. Table 14 compares individual-ion benthic-chamber measurements with the gradient-calculated fluxes.

The most obvious feature of the comparison is that the benthic chambers measured a flux of calcium and sodium 80 times greater, a flux of potassium and magnesium 120 times greater, and a flux of ammonium 20 times greater than the gradient-calculated fluxes. Note, however, that the order of the sizes of the fluxes of the individual ions is the same in the benthic chambers and in the gradient-calculated fluxes, suggesting that the same processes operating at different rates are generating the fluxes in both cases. An explanation for why the ratio of benthic-chamber ammonium flux to gradient-calculated ammonium flux is so much less than the same ratios for base cations is that the ammonium is being nitrified and denitrified in the benthic chamber, just as is likely to be occurring in the lake after the ammonium leaves the sediments.

Table 14. Cation flux (neq $cm^{-2}day^{-1}$) comparisons for Emerald Lake

Ion	Our results[a]	Benthic chambers[b]	Ratio
NH_4^+	16.	370.	23.
Ca^{2+}	2.3	190.	83.
Na^+	1.9	160.	84.
K^+	0.67	80.	120.
Mg^{2+}	0.37	40.	110.
SBC	5.3	470.	89.

Notes:
SBC = sum of base cations
a. Emerald Lake means. See Table 6.
b. Melack et al. (1987), Table II-7, p. 87. Mean of all experiments at the 9m depth, n=8.

If the base cations were coming principally from organic matter, a hypothesis which could explain the enhanced benthic chamber fluxes is that rapid stirring in the benthic chambers resulted in the oxygenation of the sediment surface, which in turn caused rapid aerobic decomposition of organic matter, which is generally thought to be much more rapid than anaerobic decomposition (Nedwell 1984, Skopintsev 1981). If, on the other hand, the base cations are coming principally from mineral dissolution, then perhaps the benthic chambers are causing enhanced mixing in the pore waters.

The gradient-calculated fluxes must be a lower limit, since they capture only what goes on below the flux plane, which is somewhat below the sediment-water interface. It is reasonable that a large proportion of organic-matter breakdown occurs naturally at or above the sediment-water interface, since that is the locus of both the most labile organic matter and the highest oxygen levels. The benthic-chamber fluxes are likely to be an upper limit, since oxygenation of the sediment-water interface and mixing in the pore waters are probably enhanced by stirring.

Melack et al. measured the shear velocity at the sediment-water interface in the benthic chambers and on the lake bottom and from these numbers calculated boundary layer thicknesses. The shear velocities in the benthic chambers were from 6 to 14 times higher than on the lake bottom, depending on the benthic-chamber pump setting, corresponding to boundary layers that were 5 to 19 times smaller. The measured boundary layer thicknesses were roughly 1 mm in the lake and 0.1 mm in the benthic chambers.

For the products of organic matter decomposition, it is appropriate to reduce the fluxes measured in the benthic chambers by the shear-velocity ratios, as Melack et al. do for specific chamber experiments, assuming that the transport of oxygen to the sediment-water interface is the rate-limiting step in aerobic organic-matter decomposition.[12] This correction brings the gradient-calculated numbers into closer agreement by about a factor of ten. If mineral dissolution is the primary source of base cations it seems unlikely than a smaller boundary layer alone would cause such greatly enhanced fluxes. Also, if mineral dissolution is the primary source of base cations, surface effects would tend to be less important, because freshly deposited minerals would not be that much more labile than deeper minerals, at least not to the same degree as organic matter.

A back-of-the-envelope calculation can provide some insight as to the reasonableness of the various flux values. If the mean gradient-calculated carbon flux, 120nmol $cm^{-2}day^{-1}$, is multiplied by 100 (the degree of enhancement of the benthic-chamber fluxes

[12] Melack et al. state (p. 85), "Since flux is proportional to shear velocity and inversely proportional to boundary layer thickness, flux values from the benthic chamber can be corrected for artificial circulation by dividing by the appropriate factor for a pump setting (for example: 6 for 80% or 14 for 90%)." Actually, flux is proportional to the gradient at the flux plane, which, for species diffusing out of the deep sediments, will be changed only slightly by the roughly 1mm difference in boundary layer thickness that is considered here. The gradient that is changed dramatically by boundary layer thickness is that of oxygen and other electron acceptors, such as nitrate and sulfate, that are diffusing from the overlying water into the sediments. This process is appropriately modeled by a well mixed reservoir of dissolved oxygen (the overlying water) separated from the reactive substrate (the sediment) by a resistive boundary layer.

over the gradient-calculated fluxes), the result is about 100mg $cm^{-2}yr^{-1}$ of organic matter, assuming that organic carbon is 50% of organic matter. The burial rate of organic matter in Emerald Lake is about 9mg $cm^{-2}yr^{-1}$, so this scenario implies that roughly 90% of the sedimenting organic matter is mineralized before burial. This mineralization rate seems high, based on some comparisons with a variety of freshwater and marine sediments (Adams and Fendinger 1986, Nedwell 1984, Aller and Mackin 1984, Skopintsev 1981). If the factor-of-ten correction for enhanced benthic-chamber shear velocity is correct, then the numbers imply a more reasonable remineralization rate before burial of about 10mg $cm^{-2}yr^{-1}$, or 50%.

Another back-of-the-envelope check on these fluxes is how they relate to total lake volume. The various hydrologic balances that have been attempted are sufficiently uncertain that the sediment contribution to lake chemistry is not statistically distinguishable from zero. A casual look at the inflow graphs and lake chemistry graphs in Melack et al. (1987) leads to a similar conclusion: The sediments must be contributing less than 10% to total lake alkalinity. The gradient-calculated base cation flux of 5neq $cm^{-2}day^{-1}$ equates to 18.meq m^{-2} yr^{-1} or 200eq yr^{-1} for the entire lake if the sediment area is about 11,000m^2. Given a lake volume of 160,000m^3, the calculated flux of base cations amounts to 1.2μeq L^{-1} of lake water each year. Of course, since the hydraulic residence time is much less than a year, the actual contribution to an average liter of lake water

would never be this high. On the other hand, the sediment contribution to bottom water under stratified conditions would be very significant. The corrected benthic-chamber estimate of ten times the gradient-calculated flux (12μeq L^{-1}) is still reasonable: Following fall overturn after three months of stratification, the sediment contribution to lakewater base cations might be about 4μeq L^{-1}. The uncorrected benthic-chamber flux, however, does not seem reasonable: it could result in an increase of 40μeq L^{-1} after fall overturn, producing an average total alkalinity of 75μeq L^{-1}, a figure far in excess of any actual measurements.

4.3.3. Denitrification and sulfate reduction

Kelly et al. (1987) estimated denitrification rates and sulfate reduction rates as a function of the lakewater concentrations of these species, based on five lakes for nitrate and 8 lakes for sulfate. They found that the denitrification rate in neq $cm^{-2}day^{-1}$ was 2.5±0.7 times the water column concentration of nitrate in μeq L^{-1}, and the sulfate reduction rate in neq $cm^{-2}day^{-1}$ was 0.15±0.04 times the water column concentration of sulfate in μeq L^{-1}. While these rates are generalizations, they do provide order-of-magnitude estimates of these processes in the lakes of this study, as shown in Table 15.

Based on these numbers for Emerald Lake, which has an unusually high nitrate concentration, denitrification could be contributing twice the alkalinity that the gradient-calculated flux of

Table 15. Denitrification and sulfate reduction estimates, compared with mean gradient-calculated base-cation fluxes

Lake	Nitrate		Sulfate		Grad-calc'd base cation fluxes (neq $cm^{-2}day^{-1}$)
	Water col. conc. (μM)	Red'n rate (neq $cm^{-2}day^{-1}$)	Water col. conc. (μM)	Red'n rate (neq $cm^{-2}day^{-1}$)	
Eastern Brook	0.6[a]	1.5	4.[a]	0.6	8.
Emerald	4.[b]	10.	6.[c]	0.9	5.
Mosquito	2.[a]	5.	2.[a]	0.3	10.

Notes:
a. Mean of all of water column measurements in this study
b. Melack et al. (1987), Figure II-6, p. 25.
c. Melack et al. (1987), Figure II-7, p. 25.

base cations does. Denitrification would represent 20% of the sediment-related base-cation flux if the corrected benthic-chamber numbers are correct.

These numbers also suggest that, in watersheds like that of Emerald Lake that are limited by a nutrient other than nitrogen, increases in atmospheric nitrate loading would result in increases in in-lake alkalinity generation via denitrification. Additional nitrate loading would not cause an increase in sediment denitrification in Eastern Brook Lake and Mosquito Lake, which have very low nitrate levels. In these watersheds, nitrate would first be consumed by primary producers. Sulfate concentrations would have to increase to levels at which the lakes were acidified before sulfate reduction would produce even the small amount of alkalinity currently produced by deep fluxes of base cations.

4.3.4. Winter peepers and annual averages

The gradient-calculated fluxes have only been done for "summer", or open water, peepers, whose concentration profiles indicate relatively rapid transport in the bottom water. The "winter", or under-ice, peepers are characterized by relatively slow transport in the bottom water. The main reason for the transport difference is the presence of wind-generated seiches in the open-water lakes and their absence in the under-ice lakes. In the under-ice peepers, the slowness of transport in the overlying water enables us to see what is invisible in the summer peepers: the high rate of organic-matter mineralization at the

sediment-water interface. This slow transport causes reaction products to accumulate at the site of the reaction, producing the peaks visible at the sediment-water interface in the winter peepers. The slowness of transport also means than oxygen becomes depleted faster than it can be replenished by diffusion. Hence the accumulation of reduced products, such as ammonium, ferrous iron, and methane. After the depletion of oxygen, nitrate, and mangannic, ferric iron becomes the preferred electron acceptor (Berner 1980, p. 82). The presence of a reservoir of oxidized iron and labile organic matter at the sediment-water interface sustains a relatively rapid rate of mineralization even after oxygen depletion.

The development of a concentration peak at the sediment-water interface causes the diffusion of alkalinity and base cations into the sediments as well as into the water column. A similar, but weaker effect occurs during summer stratification. The concentrations of base cations in the porewater near the sediment-water interface become higher than during periods when the lake is well mixed, and the exchange sites become loaded as well. After overturn, the bottom water, which has an accumulation of nutrients and alkalinity, mixes quickly into the lake, while the sediments release their buildup of nutrients and alkalinity more slowly, probably contributing alkalinity at an accelerated rate for a few weeks after overturn. Peepers EMP4B, EMP4R, MOP4B, and MOP4R, which were sampled in mid-September and early October, had base cation fluxes more than double those of the July and August peepers (see Tables 8 to 10). So, while fluxes of base cations

decrease during stratification, after overturn the gradient across the sediment-water interface becomes abnormally high, which results in an enhanced flux into the water column until the gradients stabilize. Since these surface effects probably do not change mineralization rates in the bulk of the sediments, which are permanently anoxic, the flux swings at the sediment-water interface can be viewed as oscillations in an otherwise constant flux from the deep sediments.

4.3.5. Whole-lake flux estimates

In addition to the actual fluxes out of the sediments, two factors are of importance in determining how much influence the sediments have on lakewater chemistry. The first is the ratio of the lake volume to the sediment area. Mosquito Lake is shallow with 50% of its area covered with sediments; Emerald Lake is deep with only 40% of its area in sediments. The volume to sediment-area ratio is almost four times greater in Emerald Lake. The second factor is the hydraulic residence time. During periods of rapid flow, the sediments will have little effect on lakewater chemistry; during stagnant periods they will have a much greater effect. This factor will vary drastically over the course of a single year and also from year to year. All three of the study lakes receive most of their precipitation as snowfall, and most of their flow occurs during spring melt. During maximum melt, hydraulic residence time may be only a few days; at the end of a dry summer or in mid-winter, when inflows have ceased, it is infinite. Of course, the short annual average residence time

guarantees that the sediments of these lakes will never have longer than a few months to influence a given batch of lake water.

Whole lake estimates of sediment-related alkalinity generation are presented in Table 17. These estimates are based on the lake parameters described in Table 16. It is very difficult to estimate the uncertainty of the average annual gradient-calculated fluxes, for two reasons. The first is that seasonal sampling was limited. We took enough samples to know that seasonal variation is very high (ranging even to reversed fluxes in some under-ice conditions) but not enough samples to generate precise annual averages. The numbers we have used for our estimates are averages of fluxes calculated for open-lake conditions. Simply using the standard deviation for all the peepers is not a valid technique, because they do not represent a full sample of the annual cycle and because they lead to a contradiction: negative fluxes fall within the confidence interval generated by such a procedure, and the porewater profiles indicate unequivocally that the annual net flux into the water must be positive. The second difficulty is that spatial sampling was limited. Replicate pairs of peepers were placed 5-10 m apart in the soft sediments in the deep part of the lakes. We have assumed that our calculated fluxes apply to the whole of the region of organic sediments. We estimate a "confidence interval" of our gradient calculated fluxes as annual averages to be between half and double their stated values.

Table 16. Assumptions used to make whole-lake estimates of sediment-related alkalinity generation

Parameter	Lake		
	Eastern Brook	Emerald	Mosquito
Area (ha)	4.4	2.7	2.
Sediment area (ha)	2.2	1.1	1.
Volume (m^3)	180,000.	160,000.	40,000.
Average depth (m)	4.1	5.9	2.
Ratio of vol. to sed. area (m)	8.2	15.	4.
Average SBC in lakewater ($\mu eq\ L^{-1}$)	160.	50.	60.

Table 17. Sediment-related alkalinity generation: whole-lake estimates

Source	Lake								
	Eastern Brook			Emerald			Mosquito		
	Abs.	Norm.	%	Abs.	Norm.	%	Abs.	Norm.	%
Deep fluxes of base cations	638.	3.54	2.2	212.	1.3	2.6	439.	11.	18
Surface reactions?[a]									
Denitrification	120.	0.7	0.4	400.	2.5	5.	180.	4.6	8
Sulfate reduction	48.	0.3	0.2	36.	0.2	0.5	11.	0.3	0.5

Notes:

Abs. = absolute amount ($eq \cdot yr^{-1}$)

Norm. = normalized to lake volume ($\mu eq\ L^{-1} \cdot yr^{-1}$)

% = 100(Norm.)/(average sum of base cations in lakewater)

a. While decomposition of organic matter at the sediment-water interface may be the most important source of sediment-related alkalinity, we have no good estimate. See Melack et al. (1987).

4.4. Summary and conclusions

The major deep sediment fluxes, which this study measured, are dominated by organic-matter decomposition, resulting in fluxes of carbon dioxide, methane, and ammonium. Calculations based on measured gradients indicate that diffusive transport in freshwater sediments is significantly affected by activity coefficient gradients, coulomb forces, and complex formation.

Annual average base cation fluxes from deep sediments are roughly 8, 5, and 12 neq $cm^{-2}day^{-1}$ for Eastern Brook Lake, Emerald Lake, and Mosquito Lake. Calculated for the entire sediment area, these fluxes are 600, 200 and 400 eq yr^{-1}. Normalizing to lake volume, they are 4, 1, and 10 μeq $L^{-1}yr^{-1}$. (See Table 17.) These estimates are necessarily very rough, because of large temporal variability and limited sampling. We estimate that the "confidence interval" for these numbers ranges from one half to double the stated values. They are probably less than 10% of other watershed sources of alkalinity, except for Mosquito Lake, which is very shallow. Assuming the hydrologic residence times are roughly equal, the sediments in Mosquito Lake, the shallowest lake, have the most influence on lakewater chemistry, and the sediments in Emerald Lake, the deepest lake, have the least influence.

During periods when the hydrologic residence time is short, the sediments have very little influence. During times when the hydrologic residence time is long, they have a greater influence. During periods of summer and winter stratification, the alkalinity and nutrients released from the sediments are trapped below

the thermocline. After turnover, they mix into the rest of the lake. During stratification, the elevated concentrations in the bottom water cause elevated concentrations to develop in the porewater of the upper sediments. After turnover, the higher porewater concentrations result in higher gradients and enhanced fluxes out of the sediments, possibly for several weeks, until the porewater profiles re-equilibrate with lower concentrations in the overlying water. During winter stratification, vertical transport near the bottom is very slow, due to the absence of wind-generated seiches, and oxygen depletion results in the accumulation in the bottom water of the reduced species ammonium, methane, and ferrous iron.

4.5. References

Adams, D. D. and N. J. Fendinger, ''Early diagenesis of organic matter in the recent sediments of Lake Erie and Hamilton Harbor,'' in: *Sediments and Water Interactions*, P. G. Sly, ed., p. 305-318, Springer-Verlag, New York, 1986.

Aller, R. C. and J. E. Mackin, ''Preservation of reactive organic matter in marine sediments,'' *Earth and Planetary Science Letters*, 70: 260-266, 1984.

Andrews, D. and A. Bennett, ''Measurements of diffusivity near the sediment-water interface with a fine-scale probe,'' *Geochimica et Cosmochimica Acta*, 45: 2169-2175, 1981.

Applin, K. R. and A. C. Lasaga, ''The determination of SO4--, NaSO4-, and MgSO4 tracer diffusion coefficients and their application to diagenetic flux calculations,'' *Geochimica et Cosmochimica Acta*, 48: 2151-2162, 1984.

Applin, K. R., ''The diffusion of dissolved silica in dilute aqueous solution,'' *Geochimica et Cosmochimica Acta*, 51: 2147-2151, 1987.

Bear, J., *Dynamics of Fluids in Porous Media*, American Elsevier, New York, 1972. 764 pages.

Berner, R. A., *Early Diagenesis, A Theoretical Approach*, Princeton University Press, Princeton, New Jersey, 1980, 241 pp.

Denbigh, K., *The Principles of Chemical Equilibrium, Fourth Edition*, Cambridge University Press, New York, 1981. 494 pages.

Freeze, R. A. and J. A. Cherry, *Groundwater*, Prentice-Hall, Inc., Englewood Cliffs, N.F., 1979. 604 pages.

Hesslein, R. H., ''In situ measurements of porewater diffusion coefficients using tritiated water,'' *Canadian Journal of Fisheries and Aquatic Science*, 37: 545-551, 1980.

Kelly, C. A., J. W. M. Rudd, R. H. Hesslein, D. W. Schindler, P. J. Dillon, C. T. Driscoll, S. A. Gherini, and R. E. Hecky, ''Prediction of biological acid neutralization in acid-sensitive lakes,'' *Biogeochemistry*, 3: 129-140, 1987.

Kepkay, P. E., R. C. Cooke, and A. J. Bowen, ''Molecular duffusion and the sedimentary environment: results from in situ determination of whole sediment diffusion coefficients,'' *Geochimica et Cosmochimica Acta*, 45: 1401-1409, 1981.

Krom, M. D. and R. A. Berner, ''The diffusion coefficients of sulfate, ammonium, and phosphate ions in anoxic marine sediments,'' *Limnology and Oceanography*, 25(2): 327-337, 1980.

Lasaga, A. C., ''The treatment of multi-component diffusion and ion pairs in diagenetic fluxes,'' *American Journal of Science*, 279: 324-346, 1979.

Lerman, A., *Geochemical Processes: Water and Sediment Environments*, John Wiley and Sons, New York, 1979. 481 pages.

Li, Y. H. and S. Gregory, ''Diffusion of ions in sea water and in deep-sea sediments,'' *Geochimica et Cosmochimica Acta*, 38: 703-704, 1974.

Martell, A. E. and R. M. Smith, *Critical Stability Constants, Vol. 5: First Supplement*, Plenum Press, New York, 1982. 604 pages.

McDuff, R. E. and J. M. Gieskes, ''Calcium and magnesium profiles in DSDP interstitial waters: diffusion or reaction?,'' *Earth and Planetary Science Letters*, 33: 1-10, 1976.

Melack, J. M., S. D. Cooper, R. W. Holmes, J. O. Sickman, K. Kratz, P. Hopkins, H. Hardenbergh, M. Thieme, and L. Meeker, *Chemical and Biological Survey of Lakes and Streams Located in the Emerald Lake Watershed, Sequoia National Park*, Marine Science Institute and Department of Biological Sciences, University of California, Santa Barbara, California, 93106, February 18, 1987. Prepared for the California Air Resources Board, Contract A3-096-32.

Morel, F. and J. Morgan, ''A numerical method for computing equilibria in aqueous chemical systems,'' *Environmental Science and Technology*, 6(1): 58-67, January 1972.

Nedwell, D. B., ''The input and mineralization of organic carbon in anaerobic aquatic sediments,'' *Advances in Microbial Ecology*, 7: 93-131, 1984.

Press, W. H., B. P. Flannery, S. A. Teukolsky, and W. T. Vetterling, *Numerical Recipes, The Art of Scientific Computing*, Cambridge University Press, New York, 1986. 818 pages.

Rudd, J. W. M., C. A. Kelly, V. S. Louis, R. H. Hesslein, A. Furutani, and M. H. Holoka, ''Microbial consumption of nitric and sulfuric acids in acidified north temperate lakes,'' *Limnology and Oceanography*, 31(6): 1267-1280, 1986.

Skopintsev, B. A., ''Decomposition of organic matter of plankton, humification and hydrolysis,'' in: *Marine Organic Chemistry: Evolution, Composition, Interactions and Chemistry of Organic Matter in Seawater*, E. K. Duursma and R. Dawson, eds., Elsevier Scientific Publishing Company, New York, 1981. 521 pages. (*Elsevier Oceanography Series;* vol. 31.)

Smith, R. M. and A. E. Martell, *Critical Stability Constants, Vol. 4: Inorganic Complexes*, Plenum Press, New York, 1976. 257 pages.

Sposito, G. and S. V. Mattigod, *Geochem: A Computer Program for the Calculation of Chemical Equilibria in Soil Solutions and Other Natural Water Systems*, The Kearney Foundation of Soil Science, University of California, 1979. Department of Soil and Environmental Sciences, University of California, Riverside, California 92521.

Stumm, W. and J. J. Morgan, *Aquatic Chemistry: An Introduction Emphasizing Chemical Equilibria in Natural Waters, 2nd. ed.*, John Wiley & Sons, New York, 1981.

Thibodeaux, L. J., *Chemodynamics*, John Wiley and Sons, New York, 1979. 501 pages.

Vallentyne, J. R., *The Algal Bowl, Lakes and Man*, Department of the Environment, Canadian Fisheries and Marine Service,

Ottawa, 1974. 186 pages.